Comments on Inorganic Chemistry
Publication details, including instructions for authors and subscription information:
http://www.informaworld.com/smpp/title~content=t713455155

Oxy-hemocyanin: A Peroxo Copper(II) Complex? A Mixed-Valence Alternative View

Loeb L. Bárbara[a]; Crivelli P. Irma[b]; Andrade P. Carlos[b]
[a] Facultad de Química, P. Universidad Católica de Chile, Santiago, Chile [b] Facultad de Ciencias, Universidad de Chile, Santiago, Chile

To cite this Article Bárbara, Loeb L. , Irma, Crivelli P. and Carlos, Andrade P.(1998) 'Oxy-hemocyanin: A Peroxo Copper(II) Complex? A Mixed-Valence Alternative View', Comments on Inorganic Chemistry, 20: 1, 1 — 26
To link to this Article: DOI: 10.1080/02603599808032748
URL: http://dx.doi.org/10.1080/02603599808032748

Oxy-hemocyanin: A Peroxo Copper(II) Complex? A Mixed-Valence Alternative View

BÁRBARA LOEB L.
Facultad de Química,
P. Universidad Católica de Chile,
Casilla 306, Santiago, Chile

IRMA CRIVELLI P.
and CARLOS ANDRADE P.
Facultad de Ciencias,
Universidad de Chile,
Casilla 653, Santiago, Chile

Received May 5, 1997

In the last few years we have been studying different mixed-valence copper complexes to analyze their potentiality as bioinorganic models. In this paper the most relevant spectroscopic results obtained with our model complexes are described. Contrasting these results with the information published in literature for oxy-hemocyanin, a new model is suggested for it. Specifically it is proposed that a mixed-valence superoxo species could also be related to the hemocyanin-oxygen activation process, possibly existing in equilibrium with the peroxo species, proven to exist in oxy-hemocyanin.

Key Words: *hemocyanin, oxy-hemocyanin, mixed-valence complex, superoxo-hemocyanin, bioinorganic model, copper complex*

Comments Inorg. Chem.
1998, Vol. 20, No. 1, pp. 1–26
Reprints available directly from the publisher
Photocopying permitted by license only

1. INTRODUCTION

In the last few years we have been studying different mixed-valence (MV) copper complexes, mainly to analyze their potentiality as bio-inorganic models. Several basic aspects have also been considered.[1] In this paper a contribution to the understanding of hemocyanin, in the light of our knowledge of copper mixed-valence complexes, is presented.

(a) Hemocyanin

Three general classes of respiratory proteins have evolved: hemoglobins, hemerythrins and hemocyanins.[2] While hemoglobin is the oxygen transport iron protein in vertebrates, hemocyanin (greek for "blue bloods") plays this role in arthropods and mollusks. Hemocyanin (Hc) binds oxygen at a complex dinuclear active site containing two copper atoms directly bound by protein side chains. Some of them have also been shown to exhibit a high degree of cooperativity in oxygen binding. Due to their high M.W. the structure elucidation and characterization of their metal centers has been slow. In the last years advances have been made in the crystal structures of the spiny lobster *Panulirus interruptus*[3a] and horseshoe crab *Limulus polyphems*, the latter in its deoxygenated[3b] and oxigenated[3c] forms. Both of them are arthropod hemocyanins. Until very recently, no high resolution structure of molluskan hemocyanin had been published. M. E. Cuff and W. A. Hendrickson in the American Crystallographic Association Annual Meeting, 1995, reported the structure of the oxygenated molluskan *Octupos dofleini* hemocyanin. Differences exist between the architecture of hemocyanins of arthropod and molluskan origin, but their spectral and EPR properties are alike, suggesting similarity between their active sites. Table I summarizes their main similarities and differences. *The active site, where a pair of copper atoms coordinate to oxygen, will be the center of our interest in this Comment.*

The first Hc crystal structure which was determined was that of the arthropod *desoxi-Panulirus interruptus*, Fig. 1a.[3a,4] The active site consists of a metal center formed by two Cu(I) atoms separated by 3.8 Å. Each Cu(I) is coordinated to three imidazol groups from hystidine. The surroundings are mainly hydrophobic, and various residues of triptophane and phenylanaline type are present. Two of the imidazol groups are tightly bound (Cu–N < 2.0 Å) while the third one is weakly bound (Cu–N = 2.4–3.0 Å). It is noteworthy that contrary to what was histori-

TABLE I

Comparison between hemocyanins of arthropod and molluskan origin.

Property	Molluskan Hc	Arthropod Hc
UV-Vis (oxy-Hc)[2b]	350(~20000) 570(1000) 480(CD band)	335–340(~20000) 580–590 (800–1000) 500–510 (CD band)
EPR (oxy-Hc)	Silent	Silent
MW (kDa per Cu_2 site)	50 kDa	75 kDa
Resonance Raman (oxy)		~ 750 cm^{-1}
Number of oxygen binding sites	7–8 per subunit	1 per subunit
Primary structure	Three histidines bound to Cu_B. Three histidines bound to Cu_A, one of them involved in a thioether bridge with a cysteine.	Three histidines bound to Cu_B. Three histidines bound to Cu_A.

cally thought (because of the absence of EPR signal in oxy-Hc, ascribed to a strong antiferromagnetic coupling between the two Cu(II)), *there is no endogenous bridge present to link both Cu atoms.*

The addition of O_2 to desoxi-hemocyanin generates oxi-hemocyanin. The structure of *oxi-Panulirus interruptus* has not been determined yet, but both forms are known for arthropod *Limulus Polyphenus*. In the desoxi form of *Limulus Polyphenus* the main features of *Panulirus interruptus* are preserved, but the Cu–Cu distance is apreciably longer: 4.6 ± 0.2 Å. Upon oxygenation, the copper atoms draw significantly closer to each other, resulting in a Cu–Cu distance of 3.6 ± 0.2 Å, while the histidines move only slightly. Molecular oxygen is bound symmetrically between the two copper atoms, Fig. 1b,[2] and the two oxygen atoms lie in a plane ortoghonal to the Cu–Cu axis. This μ-η^2:η^2 geometry of oxygen binding resembles the one previously reported for two synthetic copper dioxygen complexes,[5a,b] and is different from the *cis* μ-1,2 coordination proposed up to that time, or from the crystallographic *trans* μ-1,2 structure determined for some model complexes, Fig. 1c.[5c,6] To complete the information, Table II presents a selection of bond distances for the dinuclear copper sites of the deoxygenated and oxygenated forms of *Limulus polyphemus II* and the *desoxi* form of *Panulirus interruptus*.[3c]

Regarding spectroscopic data, as was shown in Table I, the molluskan and arthropod types of Oxy-Hc show similar UV-Vis spectra with two main absorptions, at 350 and 580 nm, Fig. 2a.[7,8] *Two addi-*

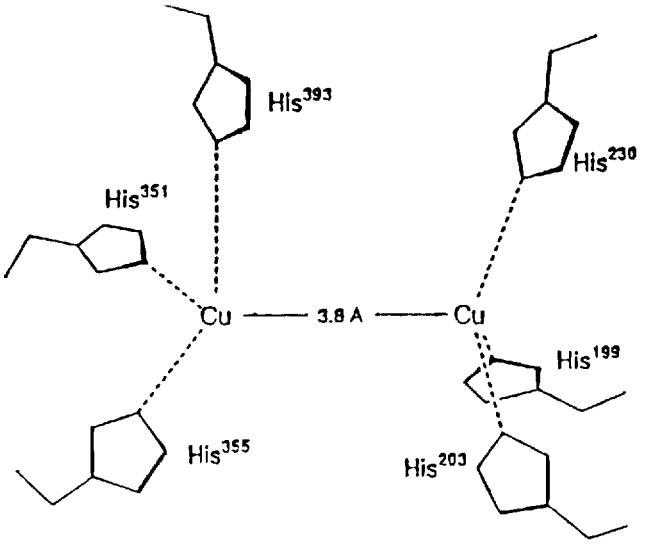

(a)

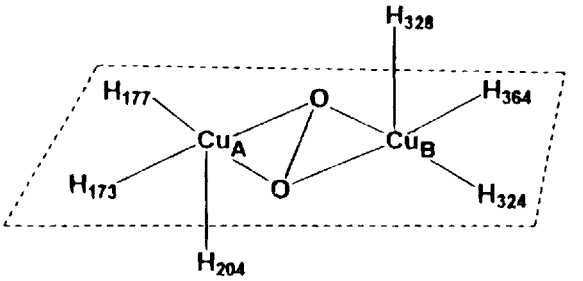

(b)

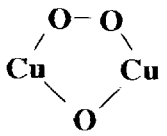

cis μ-1,2

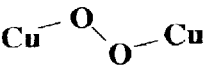

trans μ-1,2

(c)

FIGURE 1 Structure of the copper site in hemocyanin. (**a**) Copper center in *desoxi Panulirus interruptus* (Refs. 3a and 4). (**b**) Copper center in *oxy-Limulus Polyphenus* (Ref. 2). (**c**) *cis*-μ-1,2 and *trans*-μ-1,2 coordination proposed for oxy-hemocyanin (Refs. 5c and 6).

TABLE II

Selected bond distances deoxygenated and oxygenated forms of Limulus polyphemus II and the desoxi form of Panulirus interruptus.[3c]

Atoms	Lim.II deoxy	Lim.II oxy	P.int deoxy
		Distances (Å)	
N(1)–Cu(1)	2.1	2.2	2.0
N(4)–Cu(2)	2.2	1.9	2.0
N(2)–Cu(1)	2.0	2.1	2.0
N(5)–Cu(2)	2.1	2.4	2.7
N(3)–Cu(1)	1.9	2.4	2.7
N(6)–Cu(2)	1.9	2.1	2.1
Cu(1)–Cu(2)	**4.6**	**3.6**	**3.5**
O(1)–O(2)		**1.4**	
Cu(1)–O(1)		2.0	
Cu(1)–O(2)		1.7	
Cu(2)–O(1)		2.2	
Cu(2)–O(2)		2.1	

tional absorptions at 480 and 700 nm can be observed by Circular Dichroism or by lowering the temperature. On the other hand, *the Resonance Raman Spectra of the oxygenated form of these species show a band at ~750 cm^{-1}, characteristic of a peroxo group.* Therefore, the absorption bands have been assigned to LMCT $O_2^{2-} \rightarrow$ Cu(II), although the band at 350 nm has also been related to the presence of a Cu(II) dimer. In this sense, *it is amply accepted that O_2 is present in the peroxo form of Oxy-Hc; thus, by oxygenation each Cu has transferred one electron to O_2.*

Concerning hemocyanin characterization it should also be mentioned that the addition of ethylen-glycol or other alcohols to oxy-hemocyanin originates the so-called *purple hemocyanin, a violet form characterized by an absorption band at 520 nm*, Fig. 2b.[8] In this case the *Raman spectra also shows the peroxo characteristics signal at ~750 cm^{-1}, but with lower intensity.* By EPR, only 20% of the overall Cu content may be detected. A last point to be mentioned is that among Solomon's studies on half-oxidized hemocyanin,[9] some of these species, e.g., the half-met-N_3 Hc, show a broad band at ~500 nm. The assignment of this band has been rather controversial, having as possibility a $O_2^{2-} \rightarrow$ Cu(II) CT, a $N_3^- \rightarrow$ Cu(II) C.T, and also a geometrical rearrangement of the system, that would change the Cu(II) geometry to planar, displacing the absorption band, Fig. 2c.[9]

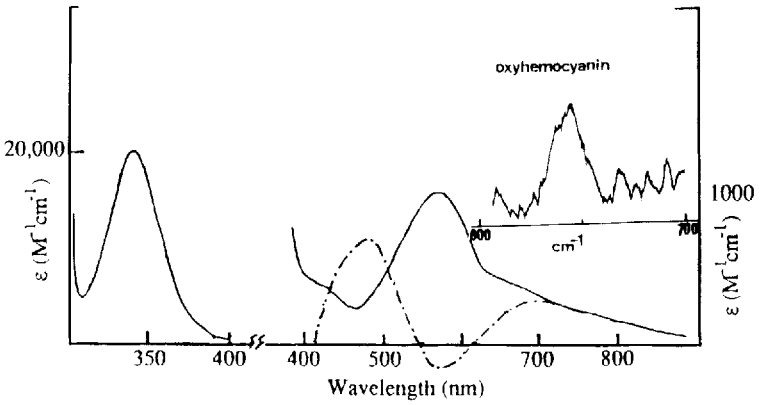

(a)

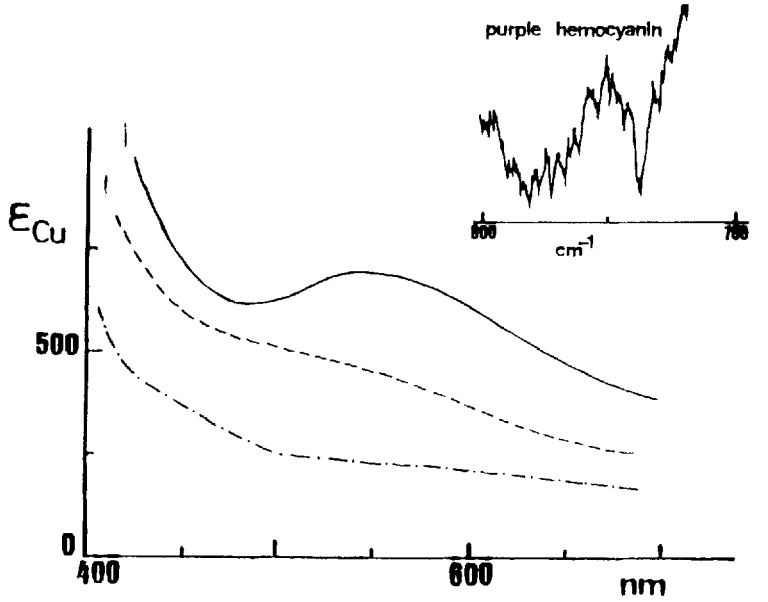

(b)

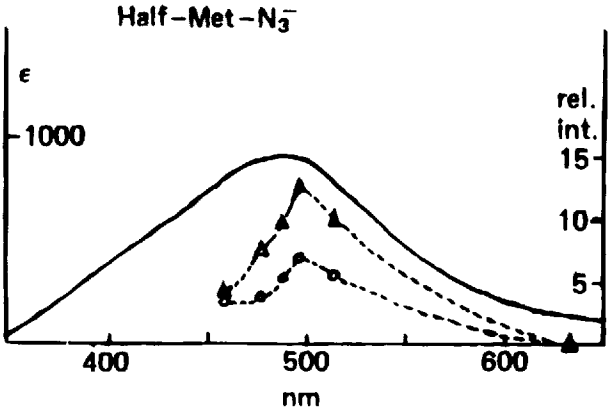

(c)

FIGURE 2 (**a**) Absorption and CD of oxy-hemocyanin (Ref. 7). Resonance Raman band shown in the inset. (**b**) Change in the absorption spectra of *oxy-Sepioteuthis lessoniana* by the addition of ethylenglycol to generate *purple* hemocyanin: 67% ethylenglycol (----); 80% ethylenglycol (——) (Ref. 8). (**c**) Optical absorption for *half-met* N_3^- hemocyanin. Resonance Raman excitation profiles indicated by dashed lines (Ref. 9).

(b) Model Compounds for Hemocyanin

Several studies have been devoted in the last decades toward model complexes for hemocyanin and their oxygenation process. Some groups to mention are Karlin's, Sorrell's and Kitajima's. The purpose of this work is not to review all of what is known with regard to Hc models, but to just point out the most relevant aspects of them, in relation to the objectives of this Comment.

As mentioned before, most of the models consider the existence of an endogenous group that would help to explain the diamagnetism of oxy-hemocyanin. Figure 3a[10] shows some of Karlin's model complexes. *Working at low temperature (–80°C), rather reversible cycles among the Cu(I)–Cu(I) synthetic derivative and the corresponding oxy-compound were observed. The latter is characterized by a violet colour and a corresponding intense band at 505 nm* (as shown in the spectrum of Fig. 3). Although with some similarities, the spectrum does not seem to correlate very well to the spectra already shown for oxy-hemocyanin. Again, Resonance Raman results show evidence of the presence of the peroxo-ion, and an electronic distribution in agreement with a Cu(II)–O_2^{2-}–Cu(II)

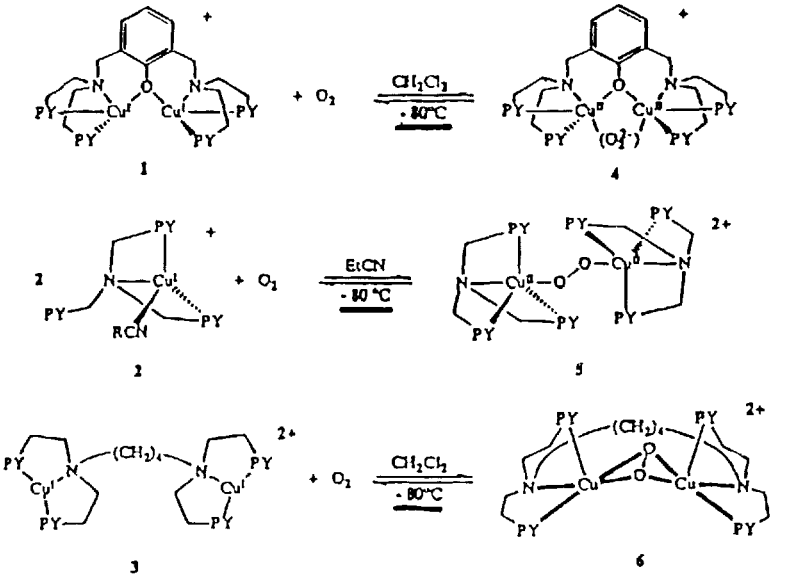

(a)

pattern. In this way, the absorption band was assigned as a peroxo → Cu(II) band. Some crystal structures have been reported for Karlin's complexes. For example, Fig. 4a shows the structure for the oxo-complex with the ligand tris[(2-pyridyl)methyl]amine, (2nd reaction in Fig. 3) where clearly a trans μ-1,2 coordination for oxygen is observed.[6] The $\nu_{O\text{-}O}$ ~803 cm^{-1} is somewhat higher than OxyHc.

On the other hand, Kitajima and his co-workers, in their widely cited 1992 JACS paper,[5a] and in preliminary notes,[5b,11] claimed to have obtained a well-characterized oxy derivative that mimics more closely the spectroscopic pattern observed for oxy-hemocyanin. The main features of these complexes were[5a]:

1. No bridging ligand besides the peroxide ion.
2. Diamagnetic behaviour.
3. $\nu_{O\ O}$ stretching frequencies in the range of 725–760 cm^{-1}.
4. According to Resonance Raman spectroscopy, a symmetric coordination of the peroxide ion was observed, as in oxy-Hc.
5. Characteristic absorption bands at ~350 (ϵ = 20000) and 550 nm (ϵ = 1000).

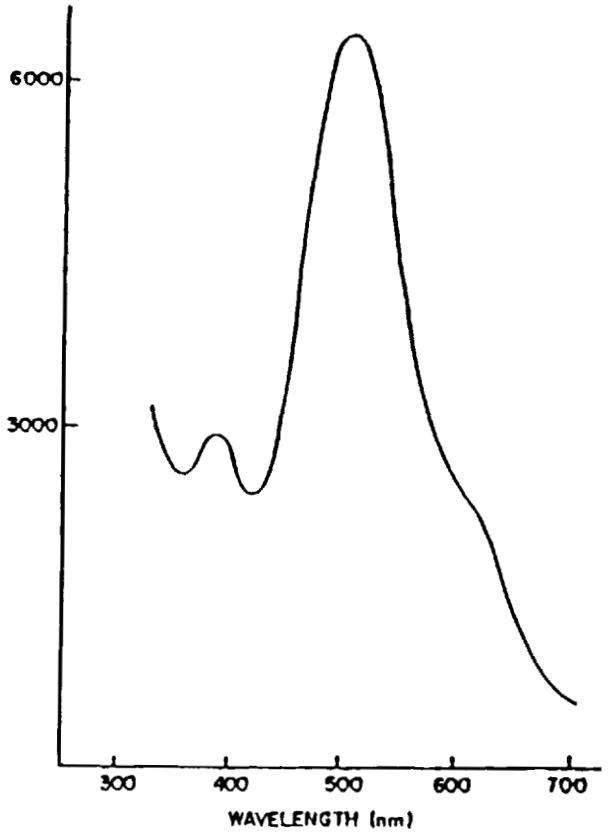

(b)

FIGURE 3 (**a**). Some of Karlin's model complexes showing reversibility towards oxygen. (**b**) Absorption spectrum for compound 4 of (**a**).

6. Absence of the Raman band assignable to Cu–O stretching vibration upon 514.5 nm excitation.
7. Cu–Cu separation of ~3.6.

The crystal structure for one of the complexes is shown in Fig. 4.[11]

All these properties have notable similarities with Oxy-Hc as may be seen from the data given in Tables I and II. Finally, Kitajima *et al.*, by simple extended Hückel MO calculations using a model $[(NH_3)_3Cu]_2$-

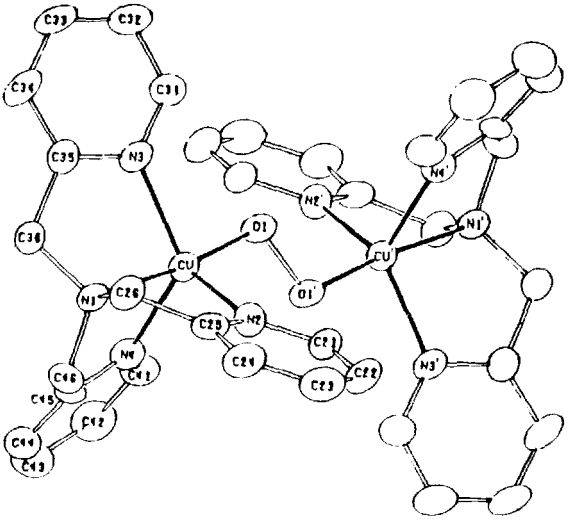

(a)

O_2^{2+} complex, explained the enhanced stability of a μ-η^2:η^2 O_2 coordination over a μ-1,2-peroxo model.

A brief summary of Hc and model complex characteristics is presented in Fig. 5.

2. COPPER-MIXED VALENCE MODELS FOR HEMOCYANIN

As mentioned before, in the last few years we have been interested in different copper mixed-valence complexes, both from a fundamental point of view and as models for hemocyanin and other copper proteins (mainly multinuclear transfer proteins).

First let us review some characteristics of mixed-valence compounds (M.V.C). In a simple way one may say that mixed-valence complexes are those that possess one element in two different oxidation states ("homonuclear" M.V.C.) or two different elements in different oxidation states ("heteronuclear" M.V.C.) Traditionally, according to Robin and Day[12a] and Hush,[12b] mixed-valence complexes have been classified into three different classes:

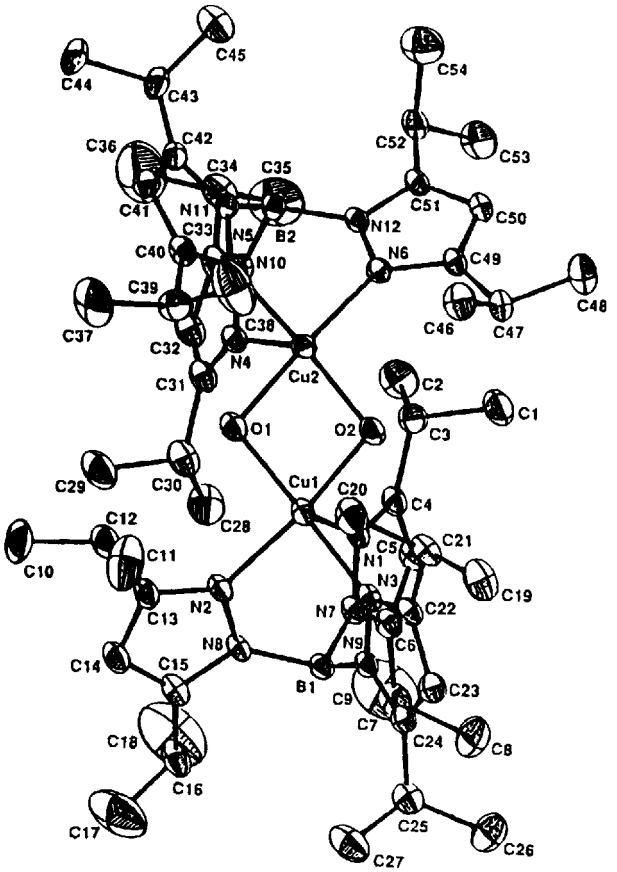

(b)

FIGURE 4 (**a**) Diagram of the structure of the peroxo dicopper(II) complex $\{(LCu)_2O_2\}^{2+}$, L = tris[(2-pyridyl)methyl]amine based on the X-ray structural determination at –90°C Ref. 6. (**b**) Ortep view of $\{Cu(HB(3,5\text{-i-}Pr_2pz)_2(OH)_2$, 30% probability (Ref. 5a).

Class I: No interaction among the metal centers. The metals show the same spectroscopic features as the corresponding monomers.

Class II: Weak interaction among the metal centers. The main physicochemical properties of the separated moieties are mantained, but new properties appear, especially a new absorption band, called *intervalence transfer band*, that represents the following process:

1). For Oxyhemocyanin, as well as for model compounds, a

$$Cu(II) - O_2^{2-} - Cu(II)$$

electronic distribution for the metal center was observed.

2). Crystal structure studies on Oxyhemocyanin, and experimental and theoretical work with models, favored a μ-η^2-η^2-peroxo coordination towards copper:

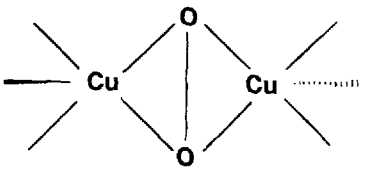

3). The absorption band at ~ 500 nm observed in some model complexes and "hidden" (detectable by circular dichroism at ~ 480 nm) in Oxyhemocyanin, was assigned to a O_2^{2-} -> Cu(II) charge transfer.

4). *The peroxo characteristic Resonance Raman band at 750 cm^{-1}* diminished its intensity by forming *purple* Hemocyanin. This last form of Hemocyanin, showed a broad absorption band at ~ 520 nm.

FIGURE 5 Summary of hemocyanin and its model complexes main characteristics.

$$M^{n+} - M^{(n+1)} \xrightarrow{h\nu} M(n+1) - M^{n+} \qquad (1)$$

Class III: Strong interaction among the metal centers. The spectroscopic properties of the individual metal centers disappear, and totally new bands appear.

It is noteworthy that mixed-valence complexes in solution are characterized by the disproportionation equilibrium described by the equation:

$$2\left[M^{n+}, M^{n+1}\right] \leftarrow K_d \rightarrow \left[M^{n+}, M^{n+}\right] + \left[M^{(n+1)}, M^{(n-1)}\right] \qquad (2)$$

The extent of the equilibrium displacement to the left or to the right depends on several factors, but mainly ΔH.

The most studied M.V. complexes have been those of Fe, Ru, etc.,[13] mainly complexes where both oxidized and reduced metal complexes have the same preferred geometric structure, so that no great structural changes are expected in going from an oxidized to a reduced form, or *vice versa*. In contrast, Cu(II) and Cu(I) have different preferred geometries, so in this case a structural change should also be considered in relation to the disproportionation equilibrium.

The synthesis of the mixed-valence copper complexes used as models was achieved in different ways, e.g., electrochemical oxidation of a Cu(I)–Cu(I) dimer,[14a] photochemical[14b] or electrochemical reduction of a Cu(II)–Cu(II)compound, or direct chemical synthesis by mixing Cu(I) and Cu(II) salts and the corresponding ligand.[14c] In what follows we will describe the main features of some of the systems studied.

(a) $[bpyCu(I)Br_2Cu(II)bpy]$[14a]

The crystal structure of $[Cu(I)(Br)(bpy)]_2$ has been reported.[15a] It proves the dimeric nature of the complex and the bridging properties of Br. The environment for both Cu(I) atoms corresponds to distorted tetrahedral, with a short Cu–Cu distance (2.86 Å). The electronic spectrum of the brown solution obtained by dissolving the reduced $[Cu(I)(Br)(bpy)]_2$ precursor in acetone shows a band at 442 nm and a shoulder at 540 nm, Fig. 6a, assigned to MLCT transitions.[15b,c] Under inert atmosphere, the complex remains as a dimer in solution, as was proven by conductivity measurements. Moreover, by cyclic voltammetry, two oxidation processes were observed, at 0.8 and 1.36 V. Electrochemical oxidation at the first oxidation peak generated a violet species after the passage of one electron, with absorption bands at 508 and 732 nm, Fig. 6b. The cyclic voltammogram of this violet species does not exhibit the first oxidation peak shown by the fully reduced precursor. After the passage of a second electron (1.36 V), a green solution remains, in which the low energy band (with an enhanced intensity) is the only one that persists.

On the basis of the observed behavior, and since the ligands undergo no electrochemical reactions in the region analyzed, both oxidations were assigned to copper centered processes:

$$[bpyCu(I)Br_2Cu(I)bpy] \longrightarrow [bpyCu(I)Br_2Cu(II)bpy]^+ + e^-$$

$$[bpyCu(I)Br_2Cu(II)bpy]^+ \longrightarrow [bpyCu(II)Br_2Cu(II)bpy]^{2+} + e^-$$

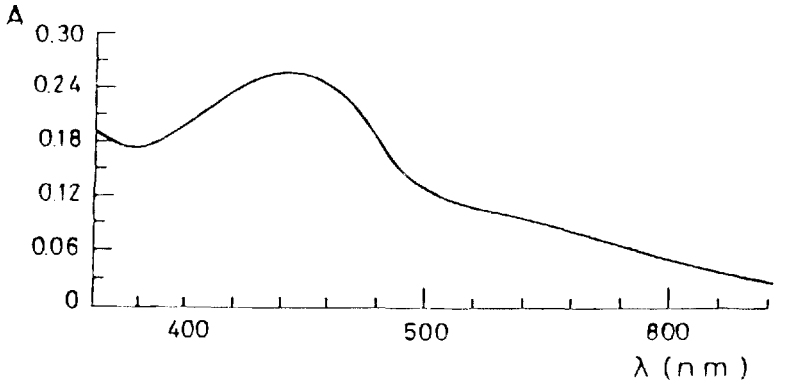

(a)

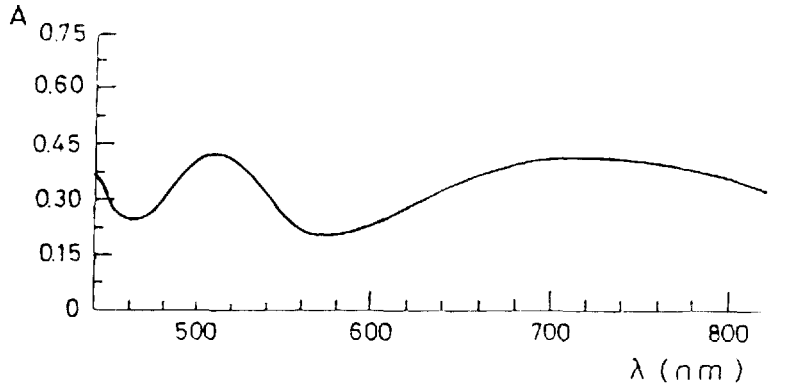

(b)

FIGURE 6 (**a**) Absorption spectrum of the reduced precursor $[Cu(I)(Br)(bpy)]_2$ in acetone (Ref. 15b,c) (**b**) Absorption spectrum of the violet complex obtained by electrolytic oxidation by one electron of the precursor in acetone (Ref. 14a).

The violet intermediate complex therefore corresponds to the mixed valence species $[bpyCu(I)Br_2Cu(II)bpy]^+$. *Its characteristic absorption band at 508 nm is absent in both, the fully reduced and the fully oxidized compounds, and may be assigned to an intervalence charge transfer band, of the type described in Eq. (1).* The high energy of this band was interpreted in this case as due to an asymmetry in the mixed-valence

complex, originated in the different preferred geometry for Cu(I) and Cu(II). The structural asymmetry should add an additional barrier to the electron transfer, therefore increasing the energy of the transition.[12b] This assumption was based also on the crystallographic information for mixed-valence copper compounds, where about 95% of the structures determined correspond to asymmetric geometries.[16]

(b) Mixed-Valence Copper–Carboxylate Complexes[14b,d]

A copper mixed-valence complex was generated photochemically from the Cu(II)–Cu(II) acetate dimer in non-aqueous solution, by irradiation with UV light in a stoppered cell.[14b] The compound obtained showed analogous optical absorption properties as the species synthesized chemically by Sigwart *et al*,[14c] starting from $Cu(I)(CH_3CN)_4ClO_4$ and $Cu(II)(ClO_4)_2$ in acetic acid–methanol solution. The UV-Vis and near IR spectrum of the $[(CH_3\text{-}COO)_2Cu(II)\text{–}Cu(I)(OOC\text{-}CH_3)_2]^-$ mixed valence complex in 95/5% (v/v) methanol–acetic acid solution, Fig. 7, *showed two new absorption bands at 508 and 960 nm, which are absent in the parent Cu(II)–Cu(II) complex.*

The EPR spectrum at room temperature of this mixed valence species generated *in situ* by UV irradiation of a Cu(II)–Cu(II) solution *showed more than the four parallel hyperfine lines* expected for Cu(II) (diamagnetic Cu(I) is EPR silent). *Specifically, seven complex lines appear,* indicating the interaction of the electron with both copper centers, therefore

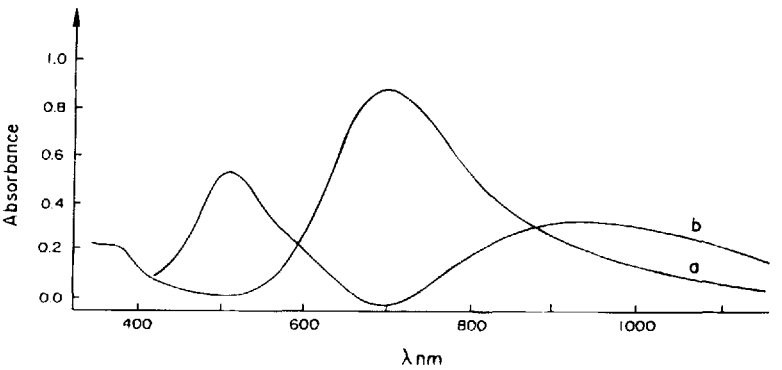

FIGURE 7 UV-Vis and NIR spectra in 95% methanol–acetic acid mixture as solvent of: (**a**) $[(CH_3\text{-}COO)_2Cu(II)]_2$. (**b**) $[(CH_3\text{-}COO)_2Cu(II)\text{–}Cu(I)(CH_3\text{-}COO)_2]^-$ generated in situ by UV irradiation of (a), taken with (a) as reference (Ref. 14b).

showing some degree of delocalization of the electron in the EPR time scale. Hush parameters[12b] were determined in order to characterize the mixed-valence complex, Table III. From the results for the half-band width $\Delta\nu_{1/2}$ and the extent of delocalization α of the electron among both copper atoms, it appears that the behavior of the near IR intervalence transfer band for the MV complex is that expected for Class II mixed valence complexes in the Robin and Day classification.[12a] Although the symmetry of the Cu(I) site in the MV species is not known, a comparison of the solid state x-ray data for the Cu(I)–Cu(I) acetate species[17c] and the corresponding Cu(II)–Cu(II) acetate dimer[17b] suggests that only a small axial distortion is expected for the Cu(I) site as compared to Cu(II), which does not imply a change in coordination number. In this way, using an orbital level scheme similar to that given for the Cu(II)–Cu(II) dimer by Hansen and Ballhausen, the low energy band at 960 nm was assigned to a transition from the state associated to the $b_\uparrow^2$ Cu(I)–$b_\downarrow^1$ Cu(II) configuration to the state associated to the $b_\downarrow^1$ Cu(II)–$b_\uparrow^2$ Cu(I) configuration. Since the 508 nm band appears only in the MV species with the typical characteristics of an intervalence transfer band, it was assigned also to an intervalence transition involving, in this case, an excited state configuration. Following Hush for a symmetric homonuclear system with a weak interaction between the metal centers, this second intervalence transfer transition may be expected to occur at an approximate frequency of $(\nu_{IT(1)} + \nu_{Cu(II)})$ with $\nu_{IT(1)}$ the fre-

TABLE III

Intervalence absorption spectral data, electronic interaction and intramolecular electron transfer parameters for $(CH_3COO)_2Cu(II)$–$Cu(I)(OOC$–$CH_3)_2$ (Ref. 14b).

	Low Energy IT Band	High Energy IT Band
ν_m[kK] (ϵ) [l mol^{-1}cm^{-1}]	19.6 (416)	10.4 (270)
$\Delta\nu_{1/2}$(Obsd) [kK]	4.0	4.0
$\Delta\nu_{1/2}$(Calc) [kK]	6.7	4.9
α	0.072	0.08
$\mathbf{V_{ab}}$[kJ mol^{-1}]	16.9	10.0
$\Delta\mathbf{G}^*$[kJ mol^{-1}][a]	165.8[b]	21.2
$\mathbf{k_{th}}$ [s^{-1}][c]	$\sim 10^{-15}$[b]	1.2×10^{9}
$\mathbf{k_{th}}$[s^{-1}][d]	9.7×10^{7}	4.0×10^{11}

[a] $\Delta G^* \sim E_{op}/4 - V_{ab}$ and $E_{op} = h c \nu_m$.
[b] Calculated considering the system as "heteronuclear" (see text).
[c] Calculated from activated complex theory, $T = 298$ K.
[d] Calculated from Hopfield, $T = 298$.

quency of the low energy IT band (960 nm) and $\nu_{Cu(II)}$ corresponding to the frequency of the internal transition of the acceptor ion (d-d transition) which is around 14 kK (700 nm). A reasonably good agreement with the experimental data was achieved with this consideration. Otherwise, *treating the 508 nm band formally as an IT band in a "heteronuclear" system where the "hetero" character is derived from* the non-equivalence of the initial and final state involved in the transition, we were able to calculate the value of ΔE between these states (thermally equilibrated states). The value 12.6 kK is on the order of the d-d internal band for Cu(II) and agrees with those expected from the Hush theory; since it was calculated independently of any transition assignation of the bands this result *gives support to the assignment of the high energy band as an IT from* $e^4b_1^2$ *Cu(I)–*b_1^1*Cu(II) to* $e^3b_1^2$ *Cu(II)–*b_1^2 *Cu(I).*

It is also worthy of mention at this point that the values estimated[14b] from the near-IR IT band, *for the electron transfer rate constant between both coppers,* k_{th}*, are of the same order of magnitude as that calculated for 1-half-met hemocyanin.*[14b,e]

Analogous results were obtained when benzoate or benzoate derivatives (orto, meta or para substituted with Cl or methyl) were used as ligands instead of acetate. The results were independent of the synthetic route used to obtain the mixed-valence complex. It is noteworthy that the band in the 500 nm region is quite insensitive to substitution on the phenyl ring, appearing always in the 514–520 nm range.

With the benzoate derivatives, some additional experiments were carried out. Figure 8 shows the absorption spectra (curve a) for the mixed-valence compound prepared with 3-chloro-benzoate as ligand,[14d] and the change in the spectrum when air is allowed to enter into the solution (see arrows). The band at 519 nm, related to the mixed-valence species, completely disappears in the presence of dissolved oxygen. Due to the isosbestic points observed, the change in the spectrum was assigned to (ligands omitted)

$$\text{Cu(I)–Cu(II)} \xrightarrow{O_2} \text{Cu(II)–Cu(II)} \qquad (3)$$

This behaviour is common to all the carboxylate systems studied.

Resonance Raman spectra[18] were registered for this mixed-valence compound, by irradiating at $\lambda = 514$ nm in methanol solution, and compared with the spectrum of the fully oxidized species. *Besides the expected carboxylate absorptions, a new signal appeared at 499* cm^{-1}*, which was related to the mixed-valence species.*

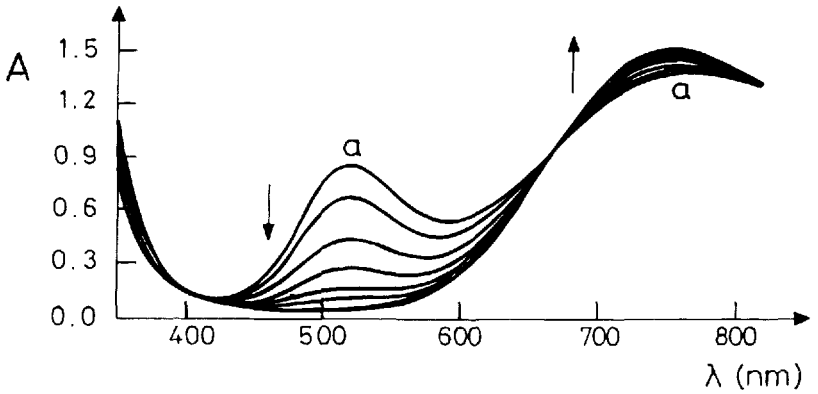

FIGURE 8 Absorption spectrum (curve a) of the mixed-valence copper complex obtained with 3-chloro-benzoate as ligand. The arrows indicate the change in the spectrum by the addition of oxygen.

For this family of mixed-valence complexes, evidence for the existence in solution of a disproportionation equilibrium of the type, ($L = C_6H_5-COO^-$, CH_3-COO^-)

$$2[\,L_2Cu(I)-Cu(II)L_2\,]^{1-} \leftarrow K_d \rightarrow [L_2Cu(I)-Cu(I)L_2]^{2-} + [\,L_2Cu(II)-Cu(II)L_2\,]^{0} \quad (4)$$

was obtained by solvent and temperature studies.[14f] In polar solvents, the neutral Cu(II)–Cu(II) species crystallizes, as proven for $L = C_6H_5-COO^-$, where the X-ray crystal[19a] structure, Fig. 9, was identical to that reported in literature for the Cu(II)–Cu(II) benzoate dimer.[19b] In non-polar solvents, a white powder corresponding to the fully reduced Cu(I)–Cu(I) complex was obtained. In both cases, as crystallization or precipitation occurs, the equilibrium is fully displaced to the right, and the mixed-valence species disappears. The temperature dependence on the equilibrium is shown in Fig. 10, for the mixed-valence complex with benzoate as ligand. At room temperature, the expected mixed-valence spectra dominates, while at 77 k the mixed-valence band in the region of 500 nm disappears, and the characteristic ligand field band in the region 650–700 nm dominates the spectrum. This effect is fully reversible, as long as no air is allowed to enter the solution. Since the Cu(I) dimer is absolutely transparent in the visible region, this effect was adscribed to a displacement of equilibrium 4 as a function of ΔH.[14f]

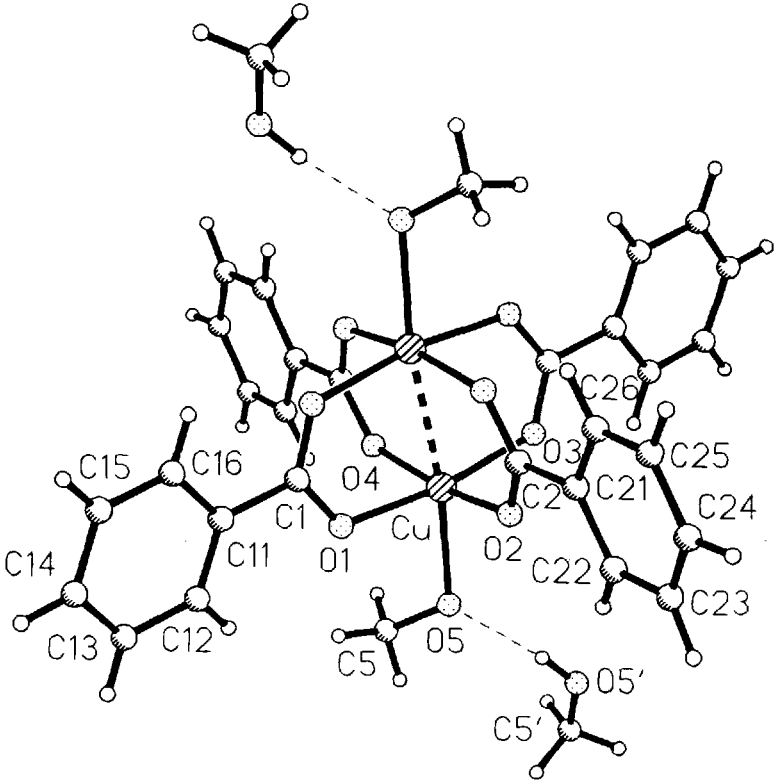

FIGURE 9 Structure of the crystals obtained from equilibrium 4, with methanol as solvent and with L = C_6H_5-COO^-.

(c) Mixed-Valence Copper–Mercaptoethylamine Complex[14a]

The synthesis of a Cu(I)–Cu(I) dimer with mercaptoethylamine (HS-CH_2–CH_2–NH_2) as ligand was achieved by the methods described by Sakurai *et al.*[20] The complex interacted with oxygen, both in solid and in aqueous solution. *In solution a violet complex merged that showed a broad absorption about 500 nm and was EPR silent. The complex was reversible towards oxygen uptake, to a certain extent:* if the solution was bubble-degassed with N_2 immediately after the appearance of the 500 nm band, the violet colour faded and the band lowered its intensity. The cycle may be repeated a couple of times, until decomposition occurs. The 500 nm band was at first related to a charge transfer band

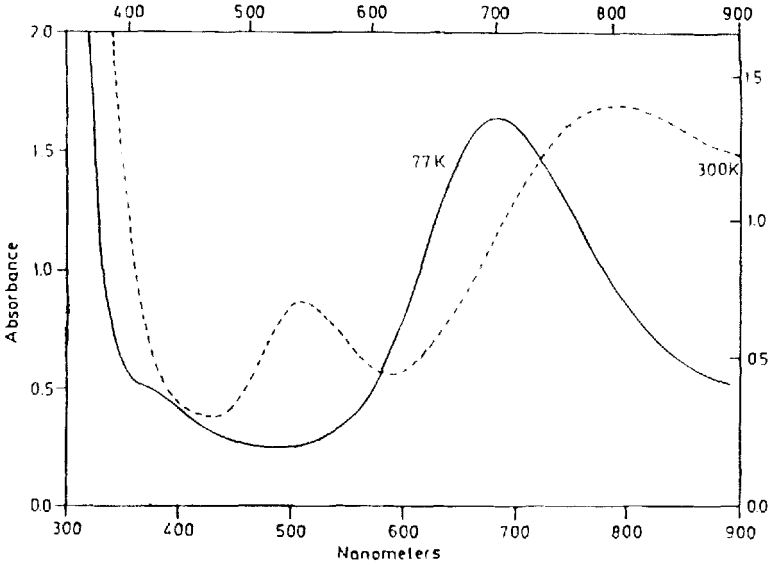

FIGURE 10 Temperature effect on equilibrium 4, for the complex obtained with L = C_6H_5-COO^-, in ethanol:methanol = 4:1 solution.

according to Karlin's model and the reversibility of the process associated to the equilibrium:

$$LCu(I)-Cu(I)L + O_2 \Leftrightarrow LCu(II)-Cu(II)L \quad (O_2^{2-})$$

It is important to mention that this was the first reported hemocyanin model where *reversible (to a certain degree) oxygen uptake was detected in aqueous solution at room temperature*.

The cyclic voltammogram of the fully reduced species, LCu(I)-Cu(I)L, shows two oxidation peaks. By electrolyzing at the first oxidation, in strict absence of oxygen, the solution turned violet and the same electronic spectrum (band at 500 nm) as that obtained by oxygen addition appeared. In the light of our previous results, *it was concluded that the violet species was a mixed-valence Cu(II)–Cu(I) species which could be achieved both by oxidizing with oxygen from air or electrolytically*. Therefore, based on these considerations and other experimental facts,[21] we proposed the following mechanism for the oxygen uptake process (ligand L omitted for simplicity):

$$\text{Cu(I)}-\text{Cu(I)} \overset{O_2}{\Leftrightarrow} [\text{Cu(I)}-\text{Cu(I)} \overset{O_2}{\Leftrightarrow} \cdots \Leftrightarrow \text{Cu(II)}-\text{Cu(I)}] \overset{O_2^-}{\rightarrow} \text{Cu(II)}-\text{Cu(I)} + O_2^-$$

where the unstable O_2^- formed disproportionates. The bracket represents the steps necessary for the gradual redistribution of the negative charge density from Cu to oxygen. As the charge transfer takes place, the appearance of a spectroscopically detectable (λ = 500 nm) mixed-valence species is observed; the irreversible loss of oxygen (as superoxide and fast subsequent dispropotionation) also occurs, and the reversibility towards oxygen is lost. If oxidation is performed electrolytically, the Cu(II)–Cu(I) compound is directly obtained.

It was suggested that the mixed-valence species described above may be associated with O_2 binding or an O_2 activation process in copper proteins, probably as a Cu(II)–Cu(I) superoxo intermediate complex. This species should also be EPR silent and have a UV-Vis spectrum similar to the corresponding Cu(II)–Cu(I) peroxo compound; moreover, both species may be present at equilibrium.

(d) Prevailing Characteristics of the Copper Mixed-Valence Complexes

Table IV summarizes the mixed-valence complexes described, and their spectroscopic characteristics. It can be seen that for a variety of bridges between the coppers and different media (solvent), where the mixed-valence complexes could be generated, a band around 500–520 nm and the characteristic violet colour are always present. This band was assigned to an intervalence transfer band for mixed-valence complexes, and it appears in most of the cases in the absence of oxygen. A Resonance Raman band at 499 cm^{-1} measured for some of these complexes was related to the presence of the mixed-valence species.

3. ARE COPPER MIXED-VALENCE COMPLEXES RELATED TO OXY-HEMOCYANIN?

As mentioned in the introduction, a *Cu(II)–Cu(I) peroxo* compound has been demonstrated to exist in oxy-hemocyanin. Based on the results described in Section 2, we tried to find out if there was any evidence for the existence of a *Cu(II)–Cu(I) superoxo* moiety in oxy-hemocyanin.

TABLE IV

Visible band for copper mixed valence complexes.

Compound	Bridge	λ max (solvent)
[CuBr(bpy)]2⁺	Halogen: Br	508 nm (Acetone)
[Cu_2(X-PhCOO)$_4$]⁻	Carboxilate	
X = H		514 nm (MeOH)*
X = CH_3 (orto)		514 nm (MeOH)
X = CH_3 (meta)		514 nm (MeOH)*
X = CH_3 (para)		514 nm (MeOH)*
X = Cl (orto)		522 nm (MeOH)
X = Cl (meta)		519 nm (MeOH)
X = Cl (para)		516 nm (MeOH)
[CU(MEA)]2⁺	Sulfur	500 nm (Water)[&]

* An additional band in the NIR (~1000 nm) is observed.
[&] Also obtained by air oxidation of the Cu^{1+}– Cu^{1+}.

(a) Resonance Raman Spectra

Larrabee *et al.*,[22a] studying oxy-hemocyanin, published a Resonance Raman spectra *where the peroxo stretching is unequivocally present at ~750 cm^{-1}*. Nevertheless *a broad Raman band was also reported at 1075 cm^{-1}*. The origin of this band was not clear, and it was attributed to a probable electronic Raman effect. *It should be remembered at this point that the superoxo anion has a Raman absorption at ~1110 cm^{-1}*.

On the other hand, Freedman *et al.*,[22b] studied in detail the O–O stretching mode assigned to bound peroxo group (745–750 cm^{-1}) in oxy-hemocyanin. Nevertheless, they also mentioned the existence of a Resonance Raman band at ~1160 cm^{-1}, *with an intensity varying according to preparation*. Maximum resonance was achieved when irradiating at 530.9 nm. The band was assigned to a covalent contaminant to hemocyanin.

Important to mention is also the fact that a *Resonance Raman band at 488 cm^{-1}* for one of Karlin's synthetic Cu(II)–Cu(II) peroxo models for oxy-hemocyanin was reported[22c] and *related to an absorption at 503 nm*. The RR band was not unambiguoslly assigned, and was associated to a probable Cu-peroxide stretching. The position of this band is very close to that reported by us at 499 cm^{-1} for the *mixed-valence* copper carboxylate complexes, *vide supra*.

In a more recent work,[22d] an extensive Resonance Raman study was reported for different hemocyanin species. A new band was identified for

Octupus mollusc oxy-hemocyanin at 542 cm^{-1} and assigned to a Cu-peroxide stretch. In this context, the band detected at 1085 cm^{-1} was related to its first overtone, allthough its intensity was much higher than that of the fundamental band. This effect was interpreted as due to the fundamental being asymmetric, while the overtone was totally symmetry allowed.

The information described in the preceeding paragraphs may be summarized as follows: *In many oxy-hemocyanins, a broad Resonance Raman band appears around 1100 cm^{-1} where superoxide absorbs.* It has not been unambiguously assigned, and it could represent a superposition of different signals. In addition, *a Cu(II)–Cu(II) peroxide reported model showed a band at 488 cm^{-1} in a position very close to the band observed for a mixed-valence benzoate copper derivative.*

(b) Other Features

(i) In early stages of the study of hemocyanin[23] a resonance between the following structures was proposed for oxy-hemocyanin:

$$\begin{aligned} \mathrm{Cu(I)-O_2-Cu(I)} &\leftrightarrow \mathrm{Cu(II)-O_2^- - Cu(I)} \\ &\leftrightarrow \mathrm{Cu(I)-O_2^- - Cu(II)} \leftrightarrow \mathrm{Cu(II)-O_2^{2-} - Cu(II)} \end{aligned}$$

Interestingly, the last structure was considered the "less probable". The electronic distribution as mixed-valence-superoxo (two middle structures) disappeared from literature in subsequent years.

(ii) Tian and Klinman[24] studied the isotope effect for reversible oxygen carriers, as hemoglobin, hemerythrin and hemocyanin. The results were related to the known crystal structure and physicochemical information available for the different carrier proteins, in order to find a relation between the structure and the isotope effects. A good correlation was observed for all of them, *except for hemocyanin*, where according to isotope effects, *the bonding to oxygen in hemocyanin should lie somewhere between the fully protonated neutral peroxide and the monoprotonated anionic peroxide.*

(iii) Baldwin *et al.*,[5c] working with the copper dimeric complex $[\{Cu(TMPA)_2\}(O_2)]^{2+}$ with TMPA = tris (2-methyl pyridyl) amine, in propionitrile at –85°C, observed an absorption band at 525 nm which was assigned to a peroxide to copper charge transfer. If the temperature was lowered to 8 K, in a mull, significant *decomposition* was observed. This result can be related to an equilibrium displacement with temperature.

(iv) Li *et al*,[25] in an abstract of a conference, suggested the possible existence of an equilibrium between peroxide and superoxide forms in an hemocyanin model. The suggestion was based on Surface Enhanced Raman Scattering (SERS) experiments for the oxygenation product of Cu_2, $(EDTB)(ClO_4)_2$ with EDTB = N, N, N′,N-tetrakis-(2-benzimidazolylmethyl)-1,2-ethanediamine. To our knowledge, this is the only report where the possibility of this equilibrium is mentioned.

CONCLUSION

Spectroscopic and crystallographic experiments with native hemocyanin and some models reported in literature have widely proven that Oxy-hemocyanin contains a $Cu(II)–O_2^{2-}–Cu(II)$ *center.*

On the other hand, based on our experimental work, we have presented here an *alternative model that reproduces some of the spectral characteristics of oxy-hemocyanin, which was characterized as a mixed-valence* $Cu(II)–O_2^-–Cu(I)$ *species.*

In this context, we propose here that a mixed-valence superoxo species could also be related to the hemocyanin-oxygen activation, possibly existing in equilibrium with the peroxo species:

$$Cu(II)–O_2^{2-}–Cu(II) \leftrightarrow Cu(II)–O_2^-–Cu(I) \qquad (5)$$

The equilibrium is probably displaced towards the peroxo derivative and consequently the spectra of the superoxo complex is masked by that of the peroxo species; then, it is understandable that in the UV-Vis spectra the absorption at 490 nm in oxy-hemocyanin could only be detected by circular dichroism. According to our results, this band could be related to the Cu(II)–Cu(I) moeity. In the Raman spectra of oxy-hemocyanin, the band at 1100 cm^{-1} could be the superposition of a superoxo absorption and an overtone of the Cu-peroxide stretching. The presence of the equilibrium (5) may justify the fact that in Freedman *et al.* studies[22b] the intensity of this band varied from preparation to preparation. Furthermore, in the work of Ling *et al.*[22d] it may also explain the higher intensity of the band assigned to a first overtone compared to the fundamental transition.

If the proposed equilibrium exists, it is very probable that by crystallization only the less soluble species crystallizes, i.e., the peroxo form of hemocyanin.[3b,c] This would be similar to the case described above for the

benzoate Cu mixed valence complex, where the Cu(II)–Cu(II) species was obtained by crystallization. Whereas crystallization selects the least soluble species from a solution, this need not correspond to the most active species and certainly need not be the only reactive one. On the other hand, considering equilibrium (5), the appearance of purple hemocyanin[8] may be seen as the displacement of this equilibrium towards the mixed valence state (superoxo species) due to a solvent effect. In this sense, the band observed for purple hemocyanin[8] in the region around 500 nm could represent an enhancement of the 490 nm masked band in hemocyanin.

We consider that the results and the proposition presented here allow a new insight into the interaction of metal complex and oxygen and has important mechanistic implications for the uptake of oxygen by hemocyanin. It may be important to identify whether or not a mixed-valence superoxo species exists as a moiety, or is present in an equilibrium with other species, in hemocyanin oxygen uptake processes. In this context, new experimental and theoretical approaches should be undertaken.

Acknowledgments

This work was supported in part by Fondecyt (Grants 0643/89 and 0831/92), Universidad de Chile (Grants Q948-855, Q949-855 and 3066-9223) and P. Universidad Católica de Chile (Grant 206/86).

References

1. (a) B. Loeb, in "Mixed Valency Systems. Applications in Chemistry, Physics and Biology", K. Prassides (ed), page 425 (1991).
   (b) A. M. Haberland, E. Hunt, A. Francois and B. Loeb, XXIX ICCC Lausane. Switzerland (1992).
   (c) See Ref. 14a, b, f.
2. (a) K. A. Magnus, H. Ton-That and J. E. Carpenter, Chem. Rev. **94**, 727 (1994).
   (b) See Ref. 22d.
3. (a) A. Volbeda and W. G. J. Hol, J. Mol. Biol. **209**, 249 (1989).
   (b) B. Hazes, K. A. Magnus, C. Bonaventura, J. Bonaventura, Z. Dauter, K. H. Kalk and W. G. J. Hol, Protein Sci. **2**, 576 (1993).
   (c) K. A. Magnus, B. Hazes H. Ton-That, C. Bonaventura, J. Bonaventura and W. G. J. Hol, Proteins: Structure, Function and Genetics **19**, 302 (1994).
4. (a) W. P. J. Gaykema, W. G. J. Hol, J. M. Vereijken, N. M. Soeter, H. J. Bak and J. J. Beintema, Nature **309**, 23 (1984).
   (b) A. Volbeda, *et al.*, in "Oxidases and Related Redox Systems", T. E. King, *et al.* (eds.), Alan R. Liss Inc., New York, p. 291 (1988).
5. (a) N. Kitajima, K. Fujisawa, C. Fujimoto, Y. Moro-oka, S. Hashimoto, T. Kitagawa, K. Toriumo, K. Tatsumi and A. Nakamura, J. Am. Chem. Soc. **114**, 1277 (1992).
   (b) N. Kitajama, T. Koda, S. Hashimoto, T. Kitagawa and Y. Moro-oka, J. Chem. Soc., Chem. Com. **1988**, 151 (1988).

(c) M. J. Baldwin, P. K. Ross, J. E. Pate, Z. Tyeklár, K. D. Karlin and E. I. Solomon, J. Am. Chem. Soc. **113**, 8671 (1991).
6. R. R. Jacobson, Z. Tyeklar, A. Farooq, K. D. Karlin, S. Lin and J. Zubieta, J. Am. Chem. Soc. **110**, 3690 (1988).
7. E. I. Solomon, M. J. Baldwin and M. D. Lowery, Chem. Rev. **92**, 521 (1992).
8. W. Mori, S. Suzuki, M. Kimura, Y. Sugiura and A. Nakahara, J. Inorg. Biochem. **13**, 89 (1980).
9. E. I. Solomon, in "Copper Proteins", T. G. Spiro, (ed.), Volume 3 of "Metal ions in Biology series", Wiley Interscience, New York, 41 (1981).
10. P. P. Paul, Z. Tyeklár, R. R. Jacobson and K. D. Karlin, J. Am. Chem. Soc. **113**, 5322 (1991).
11. N. Kitajima, K. Fujisawa, Y. Moro-oka and K. Toriumo, J. Am. Chem. Soc. **111**, 8975 (1989).
12. (a) M. Robin, P. Day, Adv. Inorg., Chem and Radiochem. **10**, 247 (1967).
(b) N. S. Hush, Prog. Inorg. Chem. **8**, 391 (1967).
13. C. Creutz, Prog. Inorg. Chem **30**, 2 (1983).
14. (a) I. Defsahut and B. Loeb, J. Coord. Chem. **33**, 33 (1994).
(b) I. Crivelli and C. Andrade, Inorg. Chim. Acta **203**, 115 (1993).
(c) C. Sigwart, P. Hemmerich and J. T. Spence, Inorg. Chem. **7**, 2545 (1968).
(d) Ref. 1b.
(e) T. D. Westmoreland, D. E. Wilcox, M. J. Baldwin, W. B. Mims and E. I. Solomon, J. Am. Chem. Soc. **111**, 6196 (1989).
(f) I. Crivelli, C. Andrade, B. Loeb and A. Francois, IV Encuentro de Quïmica Inorgánica, Antofagasta, Chile (1994).
15. (a) B. W. Skelton, A. F. Waters and A. H. White, Aust. J. Chem. **44**, 1207 (1991).
(b) S. Kitagawa, M. Munakata and N. Miyaji, Bull. Chem. Soc. Jpn. **56**, 2258 (1983).
(c) S. Kitagawa and M. Munakata, Inorg. Chem. **20**, 2261 (1981).
16. M. Dunaj-Jurco, G. Ondrejovic and M. Melnik, Coord. Chem. Rev. **83**, 11 (1988).
17. (a) R. Mounts, T. Ogura and Q. Fernando, Inorg. Chem. **13**, 802 (1974).
(b) V. M. Rao and H. Manohar, Inorg. Chim. Acta **34**, L213 (1979).
18. We thank Dr. Jon Schoonover and Dr. T. J. Meyer for the registration of the Resonance Raman spectra at UNC-Chapel Hill.
19. (a) We thank Dr. Daphne Boys for the crystal structure determination, at the University of Chile.
(b) I. Brouche-Waksman, C. Bois, G. A. Popovitch and P. L. L'Haridon, Bull. Soc. Chim. France I-69 (1980).
20. M. J. Baldwin, P. K. Ross, J. E. Pate, Z. Tyeklár, K. D. Karlin and E. I. Solomon, J. Am. Chem. Soc. **113**, 8671 (1991).
21. B. Loeb, I. Crivelli and C. Andrade, Inorg. Chim. Acta **231**, 21 (1995).
22. (a) J. A. Larrabee and T. G. Spiro, J. Am. Chem. Soc. **102**, 4217 (1980).
(b) T. B. Freedman, J. S. Loehr and T. M. Loehr, J. Am. Chem. Soc. **98**, 2809 (1976).
(c) J. E. Pate, R. W. Cruse, K. D. Karlin and E. I. Solomon, J. Am. Chem. Soc. **109**, 2624 (1987).
(d) J. Ling, L. P. Nestor, R. S. Czernuszewicz, T. G. Spiro, R. Fraczkiewicz, K. D. Sharma, T. M. Loehr and J. Sanders-Loehr, J. Am. Chem. Soc. **116**, 7682 (1994).
23. (a) C. Manwell, A. Rev. Physiol. **22**, 191 (1960).
(b) L. E. Orgel, in Crook, E. M.; "Metals and Enzyme Activity Metals and Enzyme Activity," Cambridge University Press, London, p. 19 (1958).
(c) R. Lontie and R. Witters, in Inorg. Biochem., G. L. Eichhorn, (ed.), Elsevier, Holland, Vol. 1, p. 345 (1973).
24. G. Tian and J. P. Klinman, J. Am. Chem. Soc. **115**, 8891 (1993).
25. N. C. Li, J. R. Tzou, S. W. Chen, S. M. Wang, Y. C. Chou, N. T. Liang and H. J. Lin, Recuil des Trav. Chi. Pays Bas **106**, 367 (1987).